AN EXPERIMENTAL STUDY OF TSUNAMI RUNUP ON DRY AND WET HORIZONTAL COASTLINES

Hubert CHANSON
Dept. of Civil Engineering, The University of Queensland, Brisbane QLD 4072, Australia ([1])
Fax : (61 7) 33 65 45 99 - Email : h.chanson@mailbox.uq.edu.au

Shin-ichi AOKI,
and
Mamoru MARUYAMA
Dept. of Architecture and Civil Engineering, Toyohashi University of Technology, Toyohashi, 441- 8580, Japan

ABSTRACT

Wave runup generated by a tsunami reaching the shoreline may induce devastating flood waves. When tsunami wave breaking is associated with a plunging jet, some energy dissipation at jet impact and the downstream propagation of the surge is characterised by a high initial momentum resulting from the plunging jet. New experiments were performed in a large-size facility (15-m long 0.8-m wide channel). The experimental data highlight a large wave celerity during the initial stage (i.e. $x/d_0 < 10$), followed by some deceleration caused by bottom friction and turbulent energy dissipation. The wave front travels faster than a 'classical' dam break wave because of the higher momentum of the wave. Further downstream (i.e. $x/d_0 > 30$), the bore propagates at a speed similar to that predicted by the 'classical' analysis. The results highlight a reduced warning time downstream of plunging breaking wave.

[1]Author to whom the correspondence should be adressed.

1. Introduction

1.1 Presentation

A tsunami is a long-period wave generated by ocean bottom motion during an earthquake with wave length of about 200 to 350 km. Although the wave amplitude is moderate in deep waters (e.g. 0.5 to 1 m), the tsunami wave slows down and the wave height increases near the shoreline until it breaks. The wave runup height might reach several metres above the natural sea level and cause significant damage. Major tsunami disasters were associated with well in excess of 140,000 losses of life (e.g. YEH et al. 1996, HEBENSTREIT 1997, CHANSON et al. 2000). Figure 1 shows a warning sign post along a road to the Enshu coastline, Japan. This shoreline has been historically affected by severe tsunamis. For example, the mouth of the Hamanako lake was drastically altered by a tsunami in AD 1498 (Earthquake magn. 8.6). The estuary mouth shifted by about 3.5 km and the previously freshwater lake became a saltwater system.
When the tsunami wave is slowed down by dry bed friction and overturns, the propagation of the bore on the shore is somewhat similar to the wave propagation downstream of a free-falling jet impact. For example, MURCK et al. (1997) described that Vajont dam overtopping wave as a "*tsunami-like wave*". A dominant feature of the advancing bore is its high initial momentum resulting from the breaker plunging jet. When the coastline is flat, the abnormal rise of sea level associated with the tsunami wave may runup across flat lands, sweeping away buildings and carrying ships inland. In two documented cases, the runup occurred over lakes and lagoon : i.e., at Gargano (Italy) on 30 July 1637 and at the Sissano Lagoon (PNG) on 17 July 1998 when more than 8,000 lives were lost altogether (BUTCHER et al. 1994, SARRE 1998).

Fig. 1 - Road sign post warning of tsunami danger - Takatoyo beach on the Enshu coast, Toyohashi, Japan

1.2 Analogy with dam break wave on dry and wet channels

Considering an ideal dam break surging over a dry river bed (Fig. 2A), the method of characteristics may be applied to solve completely the wave profile (e.g. HENDERSON 1966, MONTES 1998). For a horizontal rectangular channel, the shape of the ideal surge free-surface satisfies :

$$\frac{x}{t} = 3 * \sqrt{g * d} - 2 * \sqrt{g * d_o} \quad (1)$$

where the longitudinal origin (x = 0) is the dam location, t is the time, the time origin (t = 0) is the instantaneous dam break, d is the flow depth and d_o is the initial reservoir water depth (Fig. 2A). After dam break, the flow depth and discharge at the origin x = 0 are constants :

$$d_{(x=0)} = \frac{4}{9} * d_o \quad (2)$$

$$Q_{(x=0)} = \frac{8}{27} * d_o * \sqrt{g * d_o} * B \quad (3)$$

and the celerity of the wave front equals :

$$C_S = 2 * \sqrt{g * d_o} \qquad (4)$$

Fig. 2 - Definition sketches
(A) Dam break wave propagation over dry channel
(B) Dam break wave propagation in a channel with an initial water depth

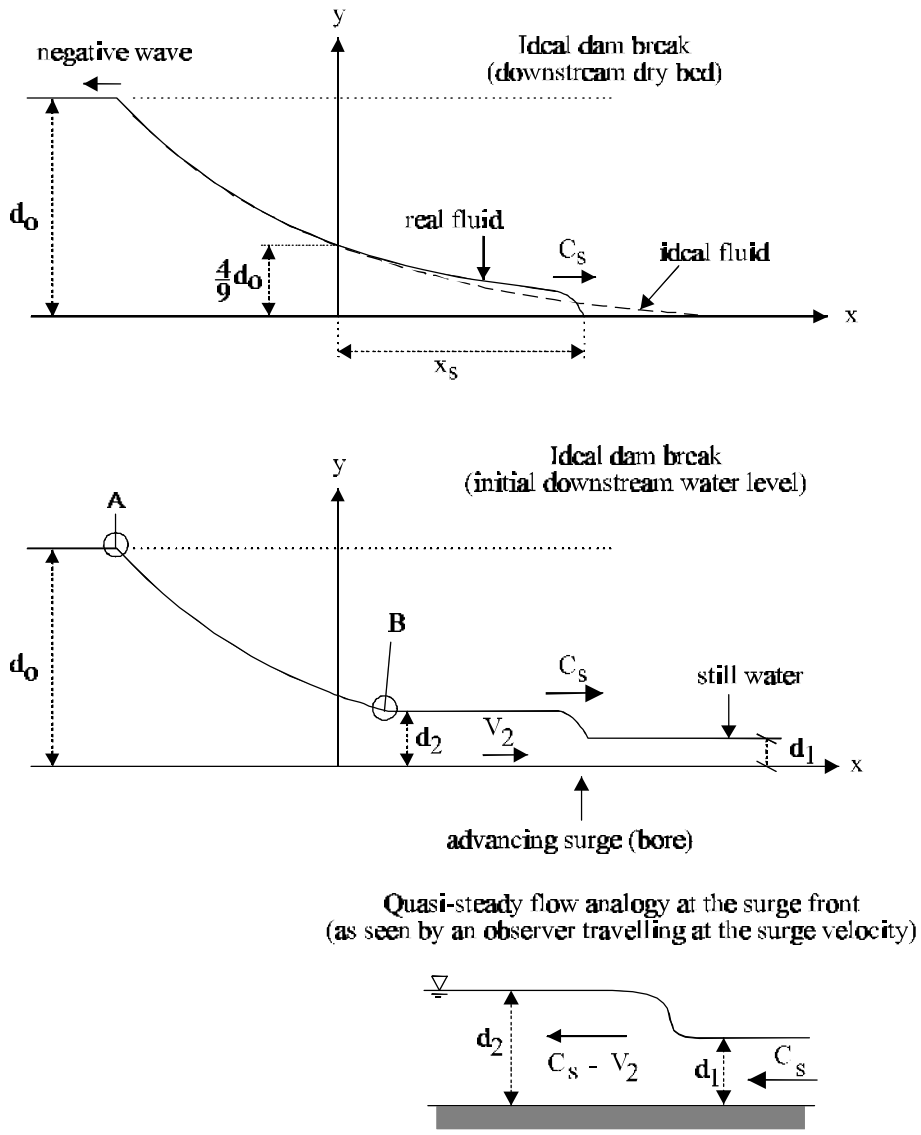

Although Equations (1) to (4) assume no boundary friction, model and prototype experiments showed good agreement with the theory, but for the leading edge of the wave (i.e. Eq. (4)). Bottom friction affects significantly the propagation of the leading tip and, taking into account the flow resistance, WHITHAM (1955) developed an analogy between the wave front and a turbulent boundary layer. For a horizontal dry channel, his estimate of the wave front celerity is best correlated by :

$$\frac{C_s}{\sqrt{g*d_o}} = \frac{2}{1.0 + 2.807 * \left(\frac{f}{8} * \sqrt{\frac{g * t^2}{d_o}}\right)^{0.425}} \quad (5)$$

with a normalised coefficient of correlation of 0.999973 and where f is the Darcy friction factor. WHITHAM (1955) commented that his work was applicable only for $C_s/\sqrt{g*d_o} > 2/3$.

The propagation of a dam break wave over still water (initial depth $d_1 > 0$) is a different situation because the dam break wave is lead by a positive surge (Fig. 2B) (HENDERSON 1966). The basic flow equations are the continuity and momentum equation across the positive surge front, and the condition along the characteristics. The system of equation may be solved graphically as (MONTES 1998) :

$$\sqrt{\frac{d_o}{d_1}} = \frac{1}{2} * \frac{C_s}{\sqrt{g * d_1}} * \left(1 - \frac{1}{X}\right) + \sqrt{X} \quad (6)$$

where

$$X = \frac{1}{2} * \left(\sqrt{1 + 8 * \frac{C_s^2}{g * d_1}} - 1\right) \quad (7)$$

Equation (6) may be correlated by ;

$$\frac{C_s}{\sqrt{g*d_1}} = \frac{0.63545 + 0.3286*\left(\frac{d_1}{d_o}\right)^{0.65167}}{0.00251 + \left(\frac{d_1}{d_o}\right)^{0.65167}} \quad (8)$$

with a normalised coefficient of correlation of 0.9999996. The flow depth downstream of (behind) the positive surge is deduced from the continuity and momentum equations (HENDERSON 1966, CHANSON 1999).

1.3 Physical modelling of tsunami wave runup

In a physical model, the flow conditions are said to be similar to those in the prototype if the model displays similarity of form, similarity of motion and similarity of forces. For free-surface flow studies, including tsunami wave runup and dam break wave, the gravity effect is usually predominant, and model-prototype similarity is performed with a Froude similitude (e.g. FAURE and NAHAS 1965, IPPEN 1966, HUGHES 1993). If the same fluids are used in both model and prototype, distortions are introduced by effects other than gravity (e.g. viscosity, surface tension) resulting in scale effects.

Considering a tsunami wave runup, bed friction opposes the fluid motion. The modelling of flow resistance is not a simple matter and often the geometric similarity of roughness height and spacing is not enough (HENDERSON 1966, CHANSON 1999). For an undistorted model, a Froude similitude implies that the model flow resistance will be similar to that in prototype if the following condition is satisfied :

$$f_R = \frac{f_p}{f_m} = 1 \quad (9)$$

where f is the Darcy friction factor, the subscripts p and m refer respectively to prototype and model flow conditions, while the subscript R refers to the ratio of prototype to model characteristics. Most prototype flows are turbulent and the model flow conditions must be turbulent : i.e., $Re_m > 5000$ to 10000 where Re is the Reynolds number.

Prototype wave runup is further characterised by significant air entrainment ('white waters') at the wave front (e.g. Fig. 4A). It is recognised that scale effects in terms of air bubble entrainment may take place with

a Froude similitude for L_R > 10 to 20, or L_R < 0.05 to 0.1 where L_R is the geometric scaling ratio (e.g. WOOD 1991, CHANSON 1997). Near the shoreline, breaking waves contribute to set sediment matters into suspension. The strong turbulent mixing, observed in the laboratory and in the field, is further enhanced by the upwelling circulation induced by the rising air bubbles. Subsequently, the combined effects of jet mixing and rising bubbles have a direct impact on the sediment transport processes (e.g. NIELSEN 1984). Physical modelling of the three-phase flow is practically impossible, but at full-scale.
Dam break wave and tsunami runup carries inland sediment materials and debris. The primary difficulty with movable-bed hydraulic models is the scaling of both the sediment movement and the fluid motion. Further the bed roughness becomes a function of the bed geometry and of the sediment transport. Several authors (e.g. HENDERSON 1996, pp. 497-508, GRAF 1971, pp. 392-398) discussed methods for 'designing' a movable bed model. CHANSON (1999, pp. 301-304) presented a detailed analysis of sediment transport modelling.

In summary, the physical modelling of tsunami wave runup in shallow waters and over dry land is very complex. In the present study, the authors investigate the wave propagation downstream of plunging jet impact in a large-size facility to minimise potential scale effects. New experiments were performed in a horizontal rectangular channel with the channel being initially dry or filled with a known water depth. The results provide new information on the energy dissipation at jet impact and on the downstream wave propagation.

2. Experimental configuration

An experimental study of wave runup downstream of plunging jet impact was conducted in a 15-m long 0.8-m wide 0.65-m deep channel (Fig. 3). The flume was horizontal and made of newly painted steel and some glass sidewall panels. The surge wave was generated by the vertical release of a known water volume through a rectangular, sharp-crested orifice (70-mm by 750 mm) at one end of the channel. A 0.5-m high sloping beach (1V:6H) was installed at the other end. The hydrograph of the free-falling jet was deduced from continuous water level measurements in the reservoir. The relationship between the tank volume and free-surface level was calibrated in-situ and the water level was measured with a capacitance wave gauge. The surging flow in the channel was studied with two video-cameras : a VHS-C camescope National™ CCD AG-30C (speed: 30 frames/sec., shutter: 1/60 & 1/1,000 sec.) and a digital handycam Sony™ DV-CCD DCR-TRV900 (speed: 30 frames/sec., shutter: 1/4 to 1/10,000 sec., zoom: 1 to 48). One camera was installed above and along the axis of the channel while the second took sideview pictures of the wave front through glass sidewall panels. Note that sideview pictures were difficult to analyse for small wave heights.

Table 1 - Summary of the experiments

Run No.	Initial volume	Head above orifice H_1	Fall height orifice-bed h	Initial water level in channel d_1	Initial discharge Q	Remarks
	m^3	m	m	m	m^3/s	
(1)	(2)	(3)	(4)	(5)	(6)	(7)
1	0.907	0.653	1.330	0.0 (*)	0.117	Run 990416_1.
2	1.031	0.740	1.330	0.0 (*)	0.124	Run 990420_1.
3	1.031	0.740	1.330	0.030	0.124	Run 990421_1.
4a	1.076	0.771	1.324	0.199	0.129	Run 990531_1.
4b	0.790	0.570	1.324	0.200	0.111	Run 990531_2.
4c	0.452	0.328	1.324	0.201	0.087	Run 990531_3.

Note : (*) : initially wet channel bed.

Fig. 3 - Experimental facility
(A) Sketch of the experiment

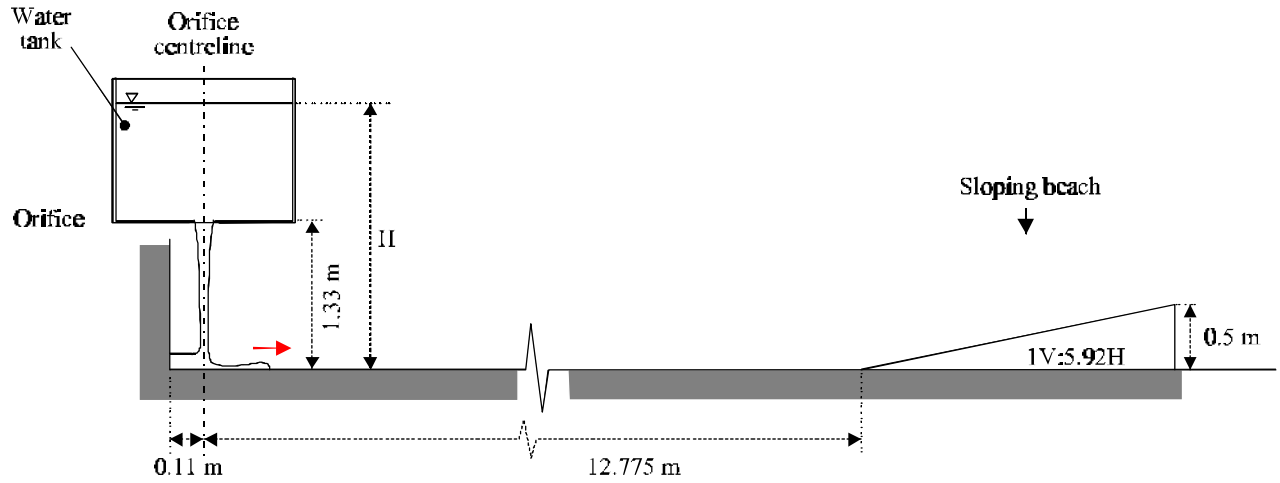

(B) Top view of the flume, with the circular water reservoir on the right of the photograph

Prior to the start of each experiment, the reservoir was filled with a known volume of water (Table 1, column 2), the orifice gate being shut. The channel was initially either dry or filled with a known water depth d_1 (Table 1, column 5). The orifice opening occurred in less than 30 milliseconds and the free-falling jet took about 260 milliseconds to reach the channel invert. The time origin (t = 0) was taken as the time of jet impact onto the channel invert or channel free-surface. The longitudinal origin (x = 0) was at the centreline of the jet. The error on the time was about 1/30 s, the error on the water depth was about +/- 1 cm and the error on the longitudinal position was +/- 2 cm. Further details on the experimental investigations were reported in CHANSON et al. (2000, 2002).
Six flow conditions were carefully documented (Table 1). In addition qualitative observations were conducted during a number of tests with initial water levels d_1 = 0 (dry channel), 0.015 and 0.3 m.

3. Experimental results

3.1 Flow patterns

Considering one single experiment, a typical sequence of events included the rapid opening of the water tank, the free-falling jet, nappe impact into the flume, the propagation of the flood wave, wave runup on the sloping beach and reflection of the wave front. Figure 4 presents typical photographs of the wave runup.

Immediately after gate opening, the free-falling jet impacted onto the channel bed or the water free-surface if the channel was initially filled with water. The initial impact was characterised by a lot of splashing and the formation of waves. (The leading wave was a positive surge when the channel was initially filled with water.) The jet impact was associated with significant energy dissipation. : i.e., the observed rate of energy dissipation ranged between 70 and 90%. The estimate was difficult because of the high level of turbulence of the surge as well as the existence of a wave front reflection on the solid boundary located at x = - 0.11 m. Following the jet impact, a wave front developed and travelled towards the downstream end of the channel (i.e. sloping beach). The wave front appeared highly aerated (e.g. Fig. 4A) for all the investigations (i.e. both $d_1 = 0$ and $d_1 > 0$). Once the wave front reached the beach, it was reflected and travelled back to the other channel end. The wave front propagation was recorded until the wave front was barely perceptible with video-camera pictures.

Fig. 4 - Wave propagation in the channel - Run No. 3, $d_1 = 0.03$ m
(A)Wave propagation (t ~ 3.5 s, x_s ~ 8 m)

(B) Wave runup on the slope beach surging to overflow the beach crest (t ~ 6 s)

3.2 Wave propagation

Figure 5 shows typical surge front data measured from the side window ($3.2 \leq x \leq 4.1$ m). The figure presents data for the first bore and the reflected bores. The horizontal time scale is in 1/30 s. For the first wave, the observed wave front shape was in agreement with the experimental data of SCHOKLITSCH (1917), FAURE and NAHAS (1961) and LAUBER (1997).

Wave front propagation speeds are presented in Figure 6. Figure 6A shows C_s/V_i where C_s is the horizontal wave front celerity and V_i is the initial jet impact velocity : i.e., $V_i = \sqrt{2*g*(H_1+h)}$. At any time $t > 0$, the jet impact velocity equals $\sqrt{2*g*(H+h)}$ where H is the total head above orifice. For $t \leq 0$, $H = H_1$. C_s was deduced from the derivative $\partial x_s/\partial t$ of the best curve fit of the data (x_s, t) where x_s is the horizontal distance between the origin and the wave front, and t is the time. The data suggest a strong deceleration in the first part of the runup up to $x/d_o = 20$ to 30, where d_o is a measure of the initial flow rate :

$$d_o = \frac{9}{4} * \sqrt[3]{\frac{Q^2}{g * B^2}} \qquad (2)$$

Q is the initial discharge (i.e. t = 0+) and B is the channel breadth. For an ideal dam break, d_o would be equivalent to the initial water level and Q would be the discharge at the origin. The present results indicate that boundary friction is significant in the first part of the horizontal runup (i.e. $x/d_o > 25$). For $x/d_o > 30$, friction losses became smaller and the wave front celerity decayed gradually. Figures 6B and 6C presents the dimensionless wave celerity $C_s/\sqrt{g*d_o}$ as a function of the dimensionless distance x/d_o. The results

show that $C_s/\sqrt{g*d_o}$ ranged from 3 down to 0.8. That is, it was significantly larger than the celerity of a dam break wave, particularly for $x/d_o < 25$.

Fig. 5 - Shape of the wave front ($x \approx 3.5$ m)
Experiment No. 3, Initial water level : $d_1 = 0.03$ m

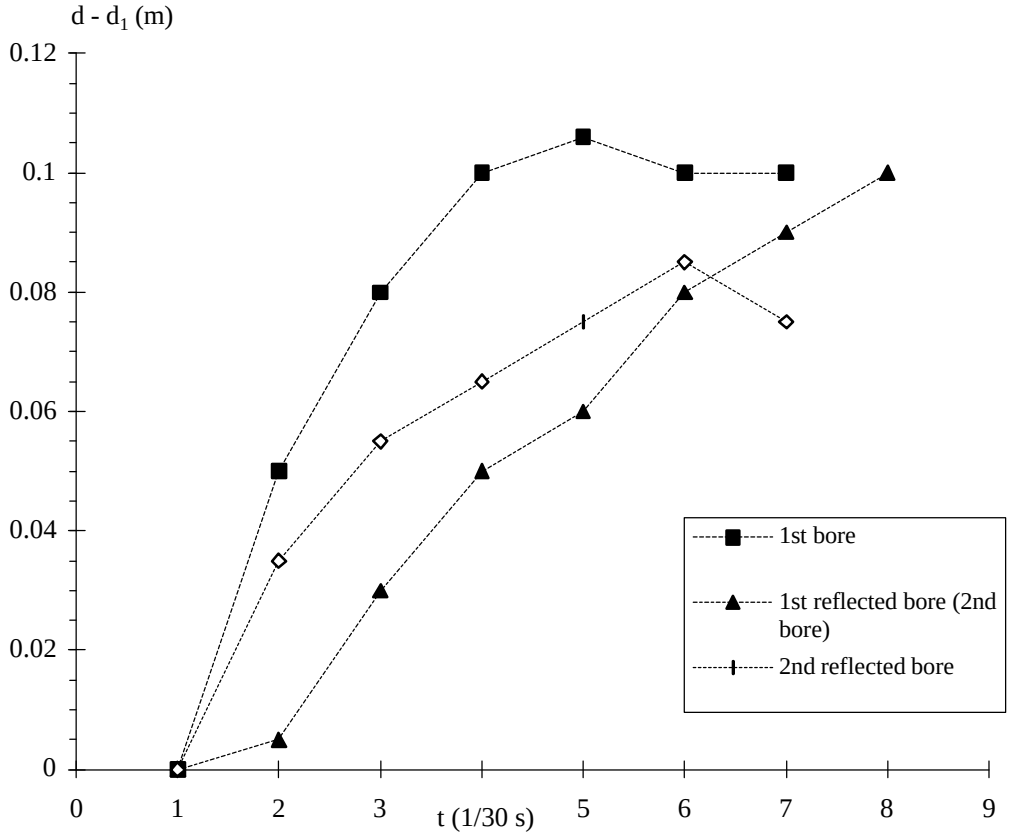

For an initial dry channel, the data (Fig. 6B) show consistently a greater wave front celerity than for the dam break analysis (WHITHAM's solution) for $x/d_o < 25$. Close to the jet impact, the wave celerity was found to be nearly twice that of the classical dam break wave (Fig. 6B). A main difference was the larger initial momentum of the wave during the present study despite significant energy loss at jet impact. The experimental data imply further a strong deceleration up to $x/d_o = 25$ to 30 (Fig. 6B). Practically the experimental data for an initially dry channel are best correlated by :

$$\frac{C_s}{V_i} = \frac{0.598}{1 - 0.0336 * \frac{x}{d_o} + 0.00237 * \left(\frac{x}{d_o}\right)^2} \quad \text{Initial dry horizontal channel } (4 < x/d_o < 30) \quad (10)$$

where V_i is the initial jet impact velocity. For $x/d_o > 30$, the agreement between the data and WHITHAM's solution is fair.

For a channel initially filled with water (Fig. 6C), the data compared favourably with the application of the momentum principle to a positive surge (HENDERSON 1966, CHANSON 1999). The results (Fig. 6C) indicated a slightly greater wave front celerity up to $x/d_o = 20$ to 25. Further downstream, the present data were consistent with the application of the momentum principle. As a first estimate, the data were best correlated by:

Fig. 6 - Propagation of the wave front

(A) C_s/V_i - Comparison with Equations (10) and (11) for dry channel and initially-filled channel respectively

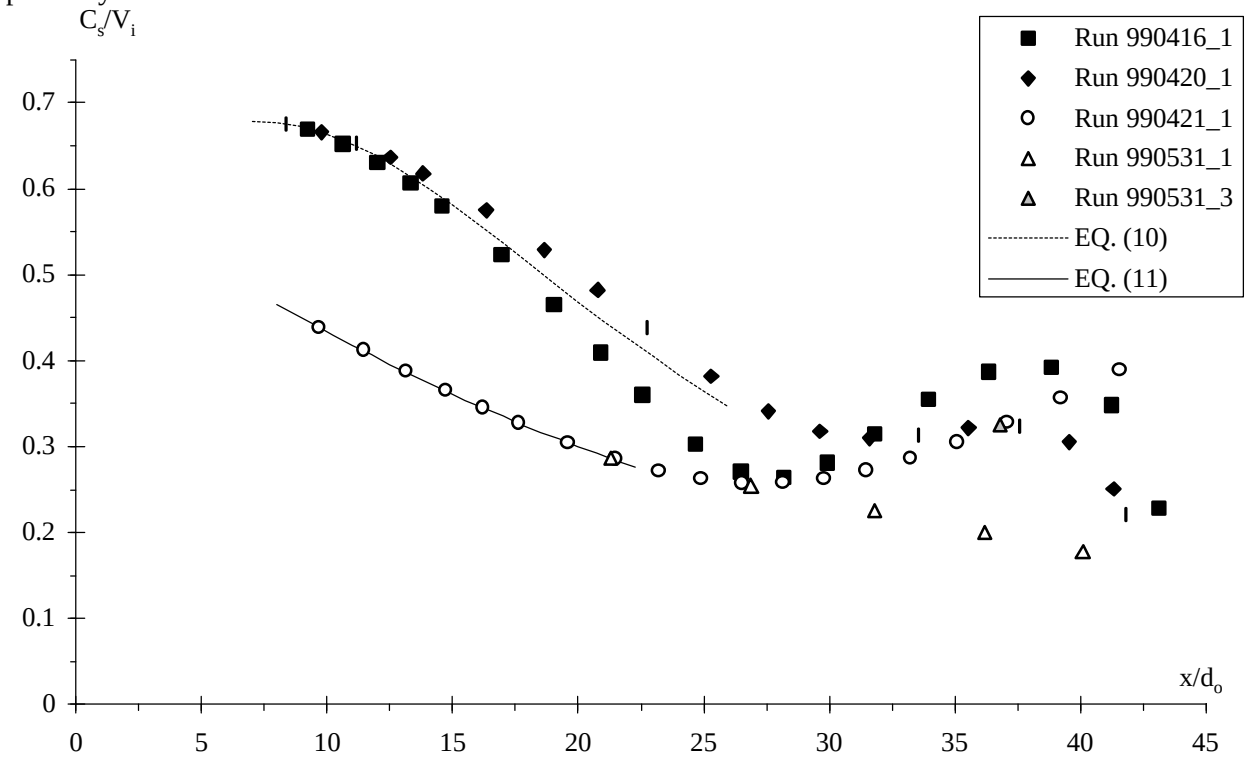

(B) $C(s)/\sqrt{g*d_o}$ (dry channel bed $d_1 = 0$) - Comparison with WHITHAM's (1955) theory

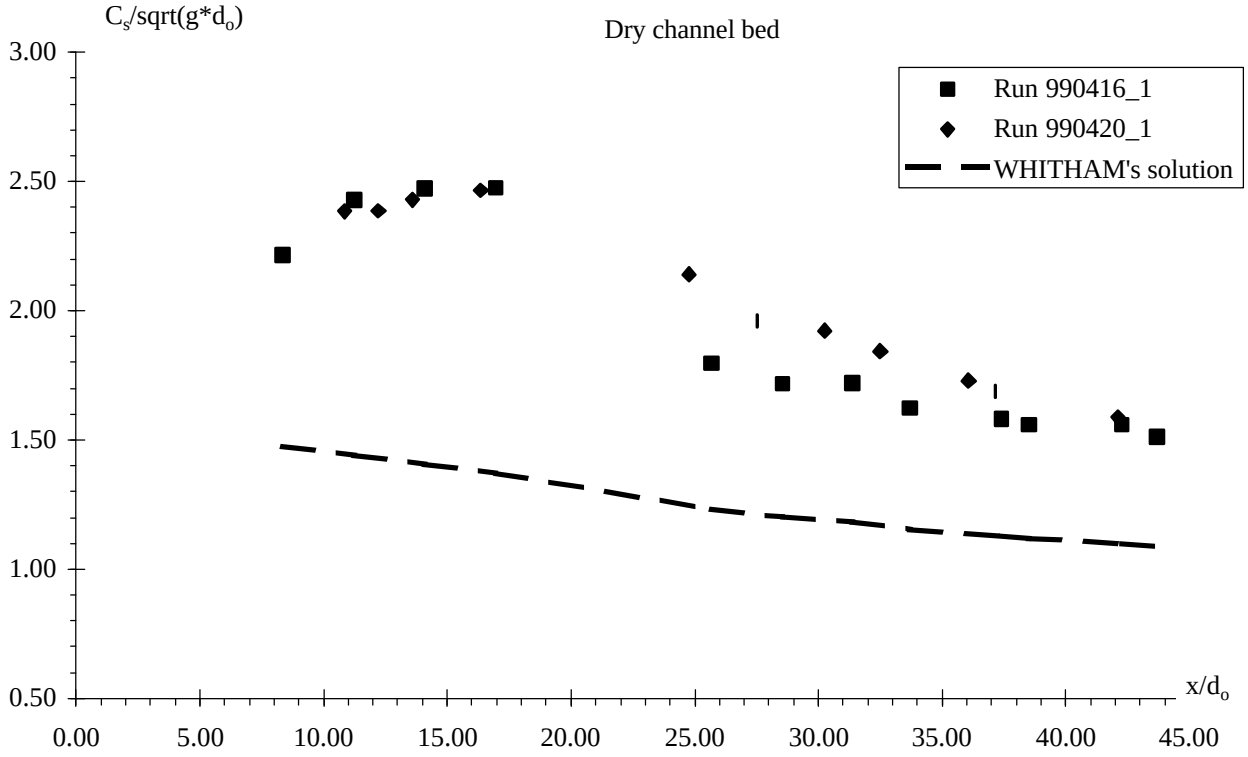

(C) C(s)/$\sqrt{g*d_o}$ (initial water depth $d_1 > 0$) - Comparison with the momentum principle

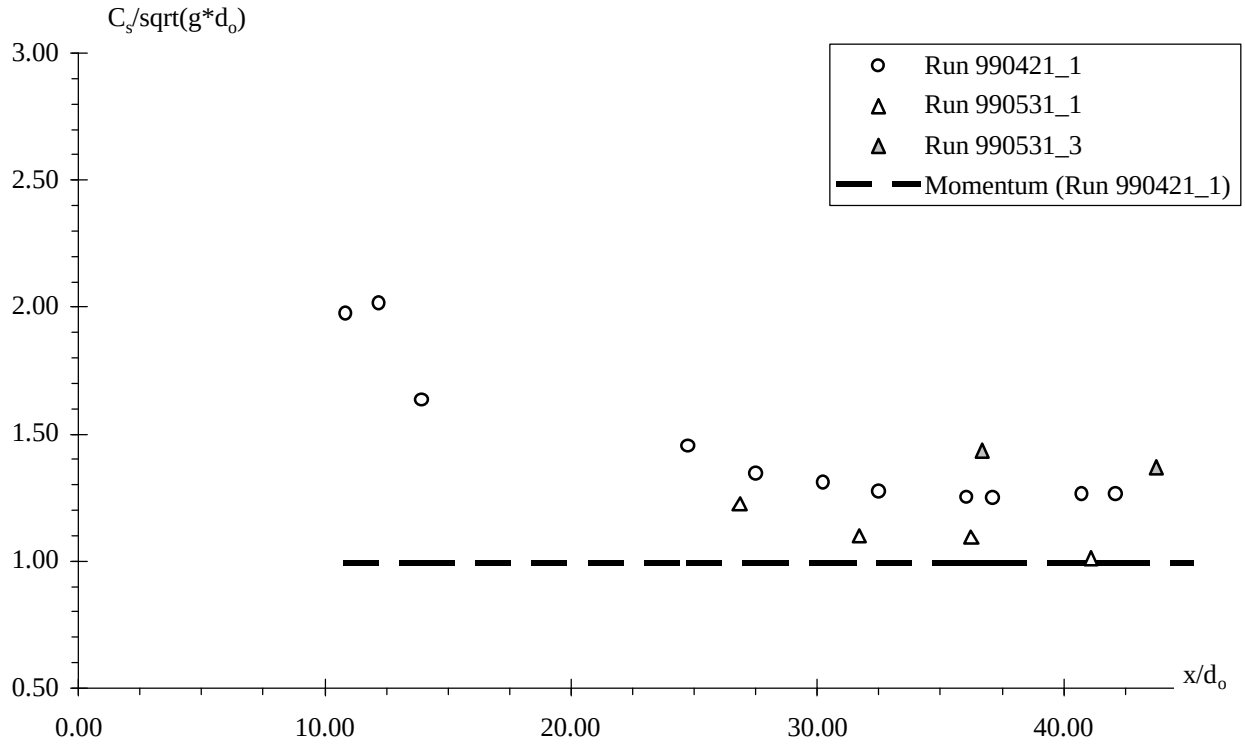

$$\frac{C_s}{V_i} = \frac{0.598}{1 + 0.0263 * \frac{x}{d_o} + 0.00117 * \left(\frac{x}{d_o}\right)^2} \qquad (0.1 < d_1/d_o < 0.8 \text{ and } 10 < x/d_o < 25) \quad (11)$$

Note that the result is little affected by the initial water depth within the range $0.1 < d_1/d_o < 0.8$.
Both Equations (10) and (11) are compared with the data in Figure 6A.

3.3 Wave runup height

The maximum runup height on the sloping beach was recorded (Table 2). For a dry channel, the initial wave runup height H_r reached about

$$\frac{H_r}{H_1 + h} \approx 0.215 \qquad (12)$$

where H_1 is the head above orifice and h is the fall height between the orifice and the channel bed. For a given experiment, the data show a decrease in the subsequent runup heights from the first (initial) bore until the third one. Once the bore become an undular surge, the energy loss is drastically reduced and the decay in runup height becomes significantly smaller.
For a channel initially filled with water, the beach was overtopped at the first runup (i.e. $H_r/(H_1+h) > 0.3$) for all investigated initial water depths, including for the smallest water depth $d_1 = 0.015$ m. The overtopping event lasted typically about 1 +/- 0.1 seconds.

Comparison with wave runup height on beaches
For non-breaking waves, the linear wave theory predicts a maximum runup height of :

$$\frac{H_r}{a} = \sqrt{\frac{2 * \pi}{\theta}} \qquad \text{Non-breaking wave (13)}$$

where a is the amplitude of the wave and θ is the beach slope in radian. For a 1:5.7 beach slope (LI and RAICHLEN 2002), the wave runup height of a solitary wave was about :

$$\frac{H_r}{d_1} \approx 3.09 * \left(\frac{H_b}{d_1}\right)^{0.95} \qquad \text{Breaking solitary wave (14)}$$

where H_b is the wave breaking height. For breaking waves, the runup height of a "surging bore" equals :

$$H_r = \frac{C_s^2}{2 * g} \qquad \text{Breaking wave (surge) (15)}$$

where C_S is the horizontal component of the bore celerity as it reaches the shore (e.g. LE MEHAUTE et al. 1968). Equation (15) would predict, within 20%, the observed runup height for the experiments with initial dry channel bed, using the observed wave front celerity. [This assumption is consistent with observations of horizontal velocity component at wave breaking by CHANSON and LEE (1997).] The same calculations (Eq. (15)) would however underestimate greatly the runup height for each experiment with initial non-zero water depth. It is suggested that the runup wave heights recorded during the present study were greater because of the high initial horizontal momentum of the bore.

Table 3-2 - Maximum surge runup height data on the sloping beach (experimental observations)

Run No.	Initial water level in channel d_1 m	Initial discharge Q m3/s	Runup height H_r m	Remarks
(1)	(2)	(3)	(4)	(5)
1	0.000	0.117	0.43	First runup.
			0.17	Second runup.
			0.11	Third runup. Undular bore.
2	0.000	0.124	0.443	First runup.
			0.17	Second runup.
			0.15	Third runup.
			0.15	Fourth runup. Undular bore.
3	0.030	0.124	> 0.5	First runup. beach overtopping for 0.9 sec.
			0.216	Second runup.
4a	0.199	0.129	> 0.5	First runup. Beach overtopping for 0.9 sec.
			> 0.5	Second runup. Beach overtopping for 1.1 sec.

4. Applications

Overall the present study shows consistently a larger wave celerity downstream of jet impact compared to a classical dam break wave. Relevant application include tsunami runup downstream of plunging breaking waves and wave runup downstream of an overtopped dam (Fig. 7). Dam overtopping may be caused by impulse waves generated by rockfalls, landslides, ice falls, glacier breakup or snow avalanches in the reservoir (e.g. Vajont dam catastrophe). Some impulse waves might be induced by earthquake-generated falls. VISCHER and HAGER (1998) gave a thorough summary of the hydraulics of impulse waves. Another cause of dam overtopping is the sudden overtopping of fully-silted reservoirs by tropical storm runoff. In South-East Australia, CHANSON and JAMES (1999) documented such fully-silted dams which are safety hazards.

For any application, the present results imply that the warning time of wave arrival is significantly smaller downstream of a falling jet than that predicted by a classical dam break wave theory.
Considering a tsunami wave (0.15 m high) generated in deep water (1000 m), the wave will break near the shore for d = 8.2 m and a wave height of 5.8 m (CHANSON et al. 2000). Assuming a plunging breaking wave, the resulting "bore" would propagate inland and Equation (10) would predict that the wave would take about 35 seconds to reach a point located 300-m from the shoreline (for a dry horizontal shore). For a bore travelling over a wet land (1-m water depth), the surge would take about 50 seconds to progress 300-m inland. Note that the latter calculations are not strictly correct because the tsunami runup was approximated by a turbulent surge while Equation (11) was deduced from experiments corresponding to a pseudo-plunging breaker.

Fig. 7 - Applications

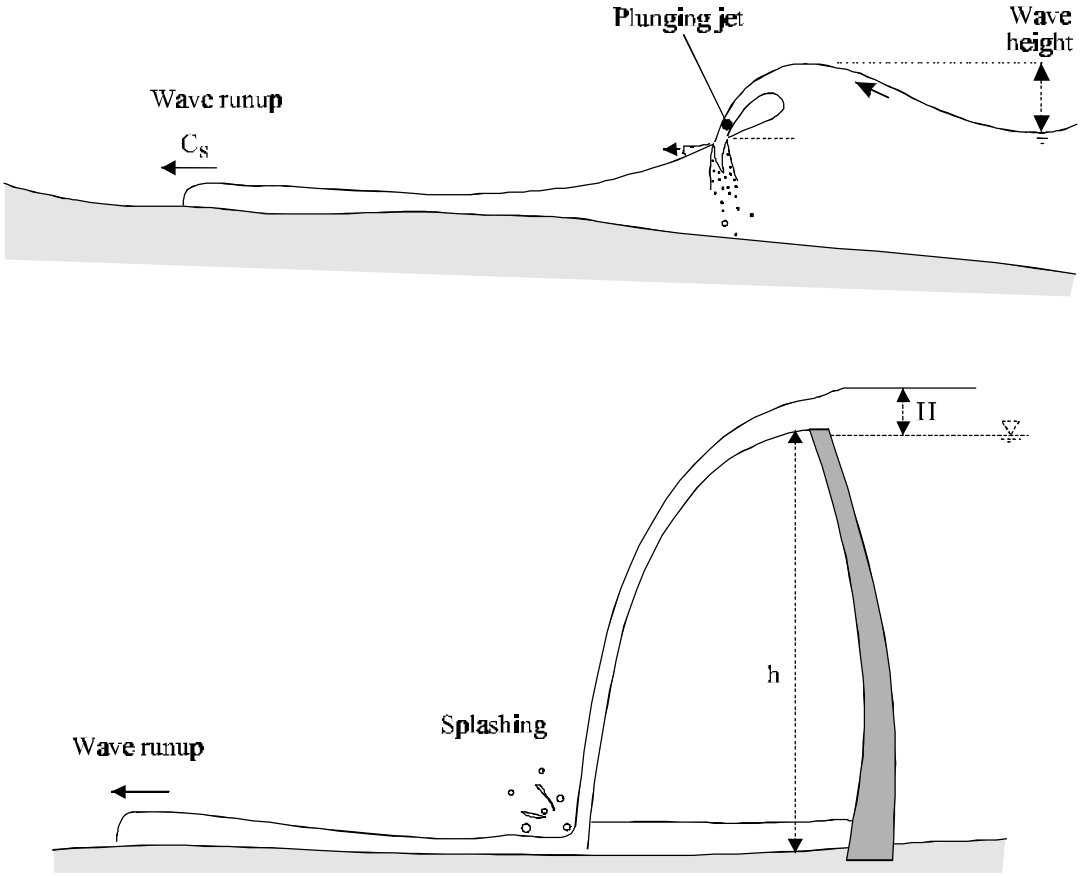

5. Summary and conclusions

This study investigates the horizontal runup of waves (i.e. bores) downstream of a free-falling jet in a large-size facility. The dominant characteristics of the advancing wave is its high initial momentum and, as a result, the wave front usually travels faster than a 'classical' dam break wave. The experimental data highlight the large wave celerity during the initial stage (i.e. $x/d_o < 10$), followed by some deceleration caused by bottom friction and turbulent energy dissipation. Further downstream (i.e. $x/d_o > 30$), the bore propagates at a speed similar to that predicted by a 'classical' analysis. New correlations (Eq. (10) and (11)) were presented to estimate roughly the wave celerity for $x/d_o < 20$ to 25.
Overall the experimental results highlight the rapid wave propagation downstream of plunging breaking waves and free-falling jets (Fig. 7). The larger wave celerity implies shorter warning times, compared to

classical dam break analysis. Further experimental work should investigate systematically the characteristics of the wave runup.

Acknowledgments

The authors acknowledge the financial support of the Australian Academy of Science, Japan Society for the Promotion of Science and Ministry of Education, Japan.

Notation

The following symbols are used in this report :

a	wave amplitude (m);
B	channel width (m);
C_s	wave front velocity (m/s);
d	water depth (m);
d_o	equivalent dam break reservoir depth (m) : $d_o = \frac{9}{4} * \sqrt[3]{\frac{Q^2}{g * B^2}}$
d_1	initial water depth (m) in the channel;
Fr	Froude number;
f	Darcy-Weisbach friction factor;
g	gravity constant (m/s^2);
H	total head above orifice (m);
H_b	breaking wave height (m);
H_r	wave runup height (m) on sloping beach;
H_1	initial total head above orifice (m);
h	fall height (m) measured from the orifice down to the channel bed;
L	length (m);
Q	total volume discharge (m^3/s) of water;
Re	Reynolds number;
t	time (s);
V	velocity (m/s);
V_i	initial jet impact velocity (m/s): $V_i = \sqrt{2*g*(H_1+h)}$;
X	dimensionless parameter;
x	horizontal longitudinal Cartesian co-ordinate (m); x = 0 at orifice centreline;
x_s	wave front coordinate (m);

Greek symbols

μ	water dynamic viscosity (Pa.s);
ν	water kinematic viscosity (m^2/s) : $\nu = \mu/\rho$;
π	π = 3.14159265358979323846264 3;
ρ	water density (kg/m^3);
$\varnothing$	diameter (m);

Subscript

R	ratio of prototype to model characteristics;
m	model;
p	prototype;
1	initial flow conditions.

References

BUTCHER, G.W., BEETHAM, R.D., MILLAR, P.J., and TANAKA, H. (1994). "The Hokkaido-Nansei-Oki Earthquake. Final Report of the NZNSEE Reconnaissance Team." *Bulletin of the New Zealand Society for Earthquake Engineering*, Vol. 27, No. 1, p. 2.

CHANSON, H. (1997). "Air Bubble Entrainment in Free-Surface Turbulent Shear Flows." *Academic Press*, London, UK, 401 pages.

CHANSON, H. (1999). "The Hydraulics of Open Channel Flows : An Introduction." *Butterworth-Heinemann*, Oxford, UK, 512 pages.

CHANSON, H., AOKI, S., and MARUYAMA, M. (2000). "Experimental Investigations of Wave Runup Downstream of Nappe Impact. Applications to Flood Wave Resulting from Dam Overtopping and Tsunami Wave Runup." *Coastal/Ocean Engineering Report*, No. COE00-2, Dept. of Architecture and Civil Eng., Toyohashi University of Technology, Japan, 38 pages.

CHANSON, H., AOKI, S., and MARUYAMA, M. (2002). "Unsteady Two-Dimensional Orifice Flow: a Large-Size Experimental Investigation." *Jl of Hyd. Res.*, IAHR, Vol. 40, No. 1, pp. 63-71.

CHANSON, H., and JAMES, D.P. (1999). "Siltation of Australian Reservoirs : some Observations and Dam Safety Implications." *Proc. 28th IAHR Congress*, Graz, Austria, Session B5, 6 pages.

CHANSON, H., and LEE, J.F. (1997). "Plunging Jet Characteristics of Plunging Breakers." *Coastal Engineering*, Vol. 31, No. 1-4, July, pp. 125-141.

FAURE, J., and NAHAS, N. (1961). "Etude Numérique et Expérimentale d'Intumescences à Forte Courbure du Front." ('A Numerical and Experimental Study of Steep-Fronted Solitary Waves.') *Jl La Houille Blanche*, No. 5, pp. 576-586. Discussion: No. 5, p. 587.

FAURE, J., and NAHAS, N. (1965). "Comparaison entre Observations Réelles, Calcul, Etudes sur Modèles Distordu ou Non, de la Propagation d'une Onde de Submersion." ('Comparison between Field Observations, Calculations, Distorted and Undistorted Model Studies of a Dam Break Wave.') *Proc. 11th IAHR Biennial Congress*, Leningrad, Russia, Vol. III, Paper 3.5, pp. 1-7 (in French).

GRAF, W.H. (1971). "Hydraulics of Sediment Transport". *McGraw-Hill*, New York, USA.

HEBENSTREIT, G. (1997). "Perspectives on Tsunami Hazard Reduction. Observations, Theory and Planning." *Kluwer Academic*, Dordrecht, the Netherlands, 218 pages. (also *Proc. 17th Intl Tsunami Symp.*, AGU, Boulder CO, USA, July 1995.)

HENDERSON, F.M. (1966). "Open Channel Flow." *MacMillan Company*, New York, USA.

HUGHES, S.A. (1993). "Physical Models and Laboratory Techniques in Coastal Engineering." *Advanced Series on Ocean Eng.*, Vol. 7, World Scientific Publ., Singapore.

IPPEN, A.T. (1966). "Estuary and Coastal Hydrodynamics." *McGraw-Hill*, New York, USA.

LAUBER, G. (1997). "Experimente zur Talsperrenbruchwelle im glatten geneigten Rechteckkanal." ('Dam Break Wave Experiments in Rectangular Channels.') *Ph.D. thesis*, VAW-ETH, Zürich, Switzerland (in German). (also *Mitteilungen der Versuchsanstalt fur Wasserbau, Hydrologie und Glaziologie*, ETH-Zurich, Switzerland, No. 152).

LE MEHAUTE, B., KOH, R.C., and HWANG, L.S. (1968). "A Synthesis on Wave Run-up." *Jl of Waterways and Harbors Div.*, Proceedings, ASCE, Vol. 4, No. WW1, pp. 77-92.

LI, Y., and RAICHLEN, F. (2002). "Non-Breaking and Breaking Solitary Wave Run-up". *Jl of Fluid Mech.*, Vol. 456, pp. 295-318.

MONTES, J.S. (1998). "Hydraulics of Open Channel Flow." *ASCE Press*, New-York, USA, 697 pages.

MURCK, B.W., SKINNER, B.J., and PORTER, S.C. (1997). "Dangerous Earth. An Introduction to Geologic Hazards." *John Wiley*, New York, USA, 300 pages.

NIELSEN, P. (1984). "Field Measurements of Time-Averaged Suspended Sediment Concentrations under Waves." *Coastal Engineering*, Vol. 8, pp. 51-72.

SARRE (1998?). "Calculating the Threat of a Tsunami." *Australian Academy of Science Nova Internet paper* {Internet address : http://www.science.org.au/nova/045/045key.htm}.

SCHOKLITSCH, A. (1917). Über Dambruchwellen." *Sitzungberichten der Königliche Akademie der Wissenschaften, Vienna*, Vol. 126, Part IIa, pp. 1489-1514.

VISCHER, D., and HAGER, W.H. (1998). "Dam Hydraulics." *John Wiley*, Chichester, UK, 316 pages.

WITHAM, G.B. (1955). "The Effects of Hydraulic Resistance in the Dam-Break Problem." *Proc. Roy. Soc. of London*, Ser. A, Vol. 227, pp. 399-407.

WOOD, I.R. (1991). "Air Entrainment in Free-Surface Flows." *IAHR Hydraulic Structures Design Manual No. 4*, Hydraulic Design Considerations, Balkema Publ., Rotterdam, The Netherlands, 149 pages.

YEH, H., LIU, P., and SYNOLAKIS, C. (1996). "Long-wave Runup Models." *World Scientific*, Singapore, 403 pages. (also *Proc. 2nd Intl Workshop on Long-Wave Runup Models*, Friday Harbour WAS, USA, Sept. 1995.)